

Stochastic Modeling of Wave Climate Using a Bayesian Hierarchical Space-Time Model with a Log-Transform

Erik Vanem* Arne Bang Huseby Bent Natvig

Department of Mathematics
University of Oslo
Oslo, Norway

Abstract

Long term trends in the ocean wave climate because of global warming is of major concern to many stakeholders within the maritime industries and there is a need to take severe sea state conditions into account in design of marine structures and in marine operations. Various stochastic models of significant wave height are reported in the literature, but most are based on point measurements without exploiting the flexible framework of Bayesian hierarchical space-time models. This framework allows modelling of complex dependence structures in space and time and incorporation of physical features and prior knowledge, yet remains intuitive and easily interpreted.

This paper presents a Bayesian hierarchical space-time model with a log-transform for significant wave height data for an area in the North Atlantic ocean. The different components of the model will be outlined, and the results from applying the model to data of different temporal resolutions will be discussed. Different model alternatives have been tried and long-term trends in the data have been identified for all model alternatives. Overall, these trends are in reasonable agreement and also agree fairly well with previous studies. The log-transform was included in order to account for observed heteroscedasticity in the data and results are compared to previous results where a similar model was employed without a log-transform. Furthermore, a discussion of possible extensions to the model, e.g. incorporating regression terms with relevant meteorological data will be presented.

1 Introduction and background

A correct and thorough understanding of meteorological and oceanographic conditions such as wind and waves, most notably the extreme values of relevant wave parameters, such as the significant wave height (H_S), is of paramount importance to maritime safety. According to the Intergovernmental Panel of Climate Change's (IPCC) Fourth Assessment Report [16, 15], the globe is experiencing climate change, and it is deemed very likely that frequencies and intensities of some extreme weather events will increase in the future. A more recent synthesis report [19] states that recent observations show that greenhouse gas emissions and many aspects of the climate are changing near the upper boundary of the IPCC range of projections. With unabated emissions, many trends in climate will likely accelerate, leading to an increasing risk of abrupt or irreversible climatic shifts. Thus, there are reasons to believe that the future climate trends will be even stronger than the projections from the IPCC report. It is not known how and to what extent such climate trends will affect the ocean wave climate and there is a need for time-dependent statistical models that can take long-term trends properly into account, along with the uncertainties in order to explore this.

*E-mail: erikvan@math.uio.no

Assuming that a significant part of the climate change is man-made and can be ascribed to the increasing emission of greenhouse gases, most notably CO₂, and aerosols, predictions of climate change can be made based on various emission, or forcing, scenarios [17, 5]. Estimates of future significant wave height (H_S) return values are difficult since there are no reliable projections of future H_S fields as pointed out by [9]. However, future return values of H_S have been projected up to 2100 in [30, 32, 31] based on regression with sea level pressure fields. The impact of climate change on extreme wave conditions, and the uncertainties involved, has also been investigated in several other studies such as [14, 12, 13], see e.g. [27] for a more comprehensive review.

A thorough literature survey on stochastic models for ocean waves, previously presented in [26, 27], identified Bayesian hierarchical space-time models as promising candidates for modelling the spatial and temporal variability of wave climate [34, 35, 10]. Thus, such a model has been developed for data of significant wave height for an area in the North Atlantic ocean as reported in [28, 29]. However, even after the seasonal component was removed, the data displayed heteroscedastic features in that more severe sea states were associated with greater variance. Hence, it might be sensible to include a log-transform in the model.

The model for significant wave height with a log-transform will be outlined herein, and the structure of the paper is as follows: The first section consists of an initial data description and inspection. The next part outlines the model that is developed. The model is hierarchical and contains different levels and components. These will be discussed, and various model alternatives will be compared. The model description will be completed in a Bayesian setting, where priors are employed in order to arrive at posterior distributions for all model parameters. The results from applying the model to data of different temporal resolution will be presented, illustrating how this may influence the results. Finally, a discussion of future extensions and improvements to the model is presented, including a discussion of possible regression terms with different meteorological data as covariates.

2 Data and ocean area used in the model

2.1 Ocean area

For the purpose of this study, an area in the North Atlantic ocean between 51°-63° North and 12°-36° West (324°-348° East) will be considered. For this area, the dataset is complete and there are no missing data. Even though this particular study is restricted to this area in the North Atlantic, it is assumed that the structure of the model will be general enough to be fitted and used in other ocean areas as well. However, the North Atlantic wave climate is often used as basis for marine design so this is a particularly interesting area to consider.

The spatial resolution of the data is $1.5^\circ \times 1.5^\circ$, hence a grid of $9 \times 17 = 153$ datapoints covers the area. Due to the curvature of the surface of the earth, the distance between gridpoints will not be constant throughout the area, but this will be ignored in this study. In particular, the distance in the longitudinal direction (East-West) differs significantly for different latitudes, see [28]. The area under consideration is indicated on a map in Figure 1.

2.2 Significant wave height data

There are many sources of data for significant wave height, as discussed in [27] but data sources with both spatial and extended temporal coverage are less numerous. In this study, the modelling has been based on the ERA-40 data of significant wave height.

The reanalysis project ERA-40 [25] was carried out by the European Centre for Medium-Range Weather Forecasts (ECMWF) and covers the 45-year period from September 1957 to August 2002. Data obtained from this reanalysis include i.a. six-hourly fields of global wave parameters such as significant wave height,

data, it may be sensible to do an initial data analysis independently in space and time, and in [28] highlights from temporal and spatial analyses of the un-transformed data were presented.

The original data were tested for normality, and such tests failed, as illustrated by the normal probability plot of all the data in figure 2. Similar tests were also performed for all data at the same locations and for all data at the same times, but neither subsets of the data were Gaussian. A few parametric distributions were also tried fitted to the data, i.e. the log-normal, Weibull, gamma, skew-normal and GEV distributions, but neither seemed to fit very well and all were rejected. In spite of being rejected by formal tests, the log-normal distribution was a better fit to the data compared to the normal distribution. Figure 2 also shows the normal probability plot of the data after a logarithmic transformation has been performed.

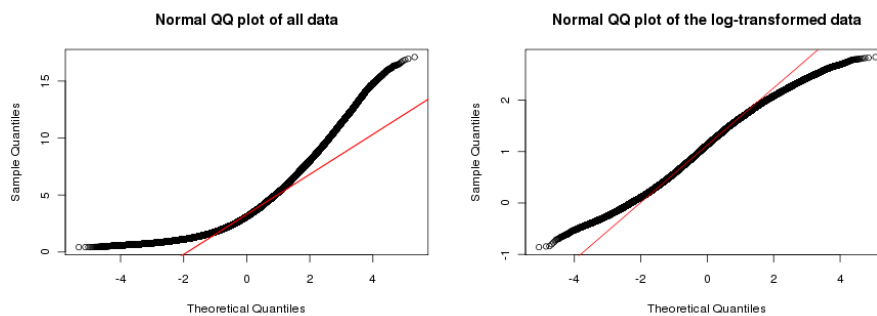


Figure 2: Normal probability plot of the data (left) and of the log-transformed data (right)

The data were also investigated for any visible detectable trends, both with respect to the temporal and spatial mean and the maxima of individual months over the period. Indications of positive trends could be seen for some months, but not for others. It was also tried to fit various simple linear regression models with the spatial coordinates as covariates, but such models were rejected due to violation of model assumptions. Finally, it is noted that the empirical mean and standard deviation in the data were 3.48 and 1.80 respectively. For more details of the initial data analysis, reference is made to [28].

There were observed some heteroscedastic features in the original time-series where the variance seems to vary seasonally. Higher significant wave heights seem to be associated with greater variance, and it is questionable whether the model without a log-transform is able to capture this satisfactorily. However, after the log-transform, the data appear to be homoscedastic and hence it is believed that the model will perform better on the log-transformed data. This is illustrated in comparing the original time series with the log-transformed time series in figure 3 with and without the seasonal mean removed. The figure for the original times series (middle) also shows the seasonal mean that was subtracted from the original data; an annual cyclic component.

Another advantage by performing a log-transform is that one does not need to worry about the possibility of estimating negative significant wave heights. This would, of course, be unphysical and any sensible model for significant wave heights should in principle be restricted from predicting negative significant wave height. However, it turned out that even with the original data this was not a major problem, with a negligible number of estimated significant wave height less than or equal to zero. At any rate, by taking the logarithmic transform this is no longer an issue. It is also interesting to note that [11] have reported good results with a log-normal transformation when modeling time series of significant wave height.

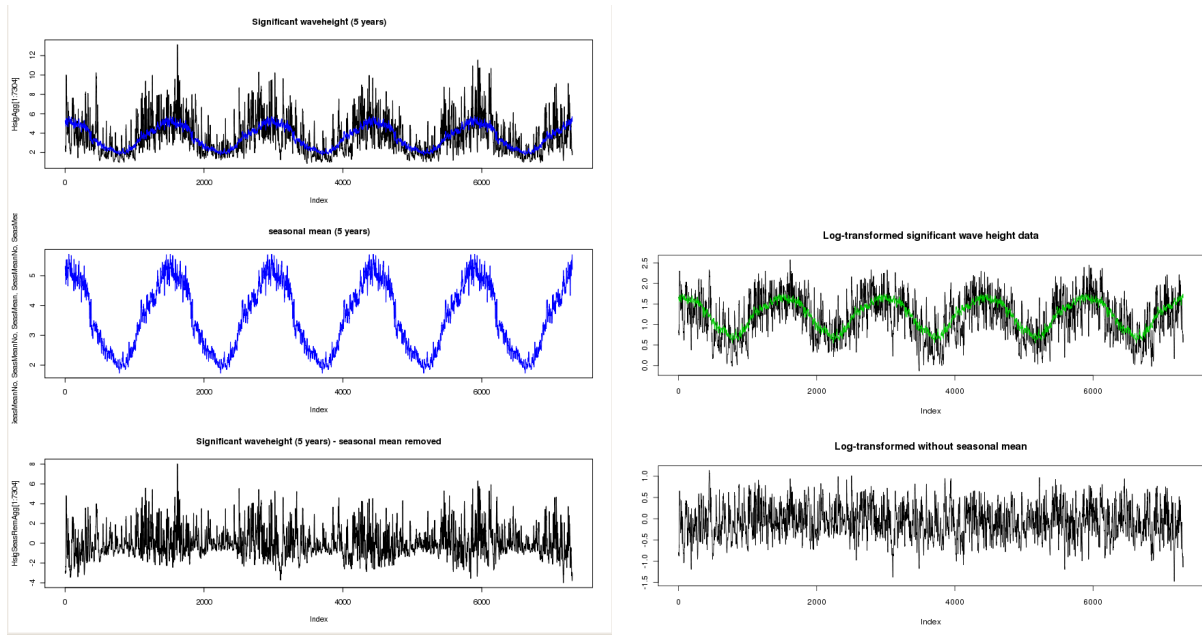


Figure 3: Time series with and without seasonal mean, original data (left) and log-transformed data (right)

3 Model description

From the initial data-inspection it is clear that the data cannot be well described by a simple Gaussian model or as a linear regression model with the spatial coordinates as covariates; a somewhat more sophisticated model must be constructed. Hierarchical models are known to model spatio-temporal processes with complex dependence structures at different scales [33]. Therefore, a Bayesian hierarchical space-time model, along the lines drawn out by e.g. [34] will be used to model the significant waveheight data in space and time.

The spatio-temporal data will be indexed by two indices; an index x to denote spatial location with $x = 1, 2, \dots, X = 153$ and an index t to denote a point in time with $t = 1, 2, \dots, T = 64\,520$. Hence, each datapoint in the rather huge set of data (nearly 10 million datapoints) are unambiguously identified by these two indices. A log-transform will be carried out so that the logarithm of the significant wave height data will be construed as the observations.

The spatial dependencies will be modelled as a Markov Random Field with dependence on nearest neighbours in all cardinal directions. The temporal dependence is modelled by three terms. Two, assumed independent in space, is included to model the strong seasonal dependence in the data and possible long term temporal trends. The last one, a short-term temporal contribution with a spatial description, is modelled as a vector autoregressive model of order one, conditionally dependent on the nearest neighbours. The model resembles the model for earthquake data presented in [18], but differs in some aspects due to fundamentally different characteristics of the underlying dynamics of earthquakes and ocean waves. Most notable, the model presented herein contains a seasonal component, which has been seen to dominate the temporal variation in the data, whereas there are no strain term similar to the strain term in the earthquake model. Furthermore, the significant wave height data is not zero-inflated; in fact, zero significant wave height is not meaningful so the significant wave height should always be strictly positive. In a sense, this simplifies the modelling, but care should be taken so that negative significant wave heights are not predicted by the model.

The structure of the model will be outlined below; first the basic or main model will be outlined, and then various model alternatives are suggested for comparison. Then possible extensions to this model are discussed, where for example different meteorological data can be used as covariates for regression.

3.1 Main model

Denoting $Z(x, t)$ the significant wave height at location x and time t , the log-transforms are first carried out for each location and time-point,

$$Y(x, t) = \ln Z(x, t) \quad (1)$$

Then, at the observation level, the log-transformed data, Y , are modelled as the latent (or hidden) variable, H , corresponding to some underlying significant waveheight process, and some random noise, ε_Y , which may be construed as statistical measurement error:

$$Y(x, t) = H(x, t) + \varepsilon_Y(x, t) \quad \forall x \geq 1, t \geq 1 \quad (2)$$

All the noise terms, in this and in subsequent components, are assumed independent in space and time, having a zero-mean Gaussian distribution with some random, but identical variance; with generic notation, $\varepsilon_N(x, t) \stackrel{i.i.d.}{\sim} N(0, \sigma_N^2)$. It is noted that all noise terms to be included in the model are assumed to be independent of all other noise terms in the model.

An equivalent representation of the observation model would be

$$Z(x, t) = e^{H(x,t)} e^{\varepsilon_Y(x,t)} \quad \forall x, t \quad (3)$$

where now the noise term has become a multiplicative factor rather than an additive term.

The underlying process for the significant waveheight at location x and time t is modelled by the following state model, which is assumed split into a time-independent component, $\mu(x)$, a temporally and spatially dependent component $\theta(x, t)$ and a spatially independent seasonal component, $M(t)$, as shown in eq. 4. A separate term is included to model long-term temporal trends, $T(t)$, which is assumed to be spatially invariant and which is, in fact, the component of most interest in this particular case. In line with the model presented in [18], no noise terms are introduced in the model at this level.

$$H(x, t) = \mu(x) + \theta(x, t) + M(t) + T(t) \quad \forall x, t \quad (4)$$

Now, the alternative representation of eq. 3 can be written as the product of five multiplicative factors and it is important to note that therefore, the contribution from each of the model components will have a somewhat different interpretation compared to the model for the original data.

$$Z(x, t) = e^{\mu(x)} e^{\theta(x,t)} e^{M(t)} e^{T(t)} e^{\varepsilon_Y(x,t)} \quad \forall x, t \quad (5)$$

The time-independent part is modelled as a first-order Markov Random Field (MRF), conditional on its nearest neighbours in all cardinal directions, and with different dependence parameters in lateral and longitudinal direction, as shown in eq. 6. For the remainder of this document, the following notation is used for neighboring locations of x in space: x^D = the location of the nearest gridpoint in direction D from x , where $D \in \{N, S, W, E\}$ and N = North, S = South, W = West and E = East. If x is at the border of the area, the value at the corresponding neighboring gridpoint outside the data area is taken to be zero. Hence, no particular adjustment is made to account for edge effects.

$$\begin{aligned} \mu(x) = & \mu_0(x) + a_\phi \left\{ \mu(x^N) - \mu_0(x^N) + \mu(x^S) - \mu_0(x^S) \right\} \\ & + a_\lambda \left\{ \mu(x^E) - \mu_0(x^E) + \mu(x^W) - \mu_0(x^W) \right\} + \varepsilon_\mu(x) \quad \forall x \end{aligned} \quad (6)$$

In the equation above, $\mu_0(x)$ is the Markov Random Field mean at grid point x and a_ϕ and a_λ are spatial dependence parameters in lateral (i.e. North-South) and longitudinal (i.e. East-West) direction respectively. σ_μ^2 is the homogeneous Markov Random Field variance. The spatially specific mean, $\mu_0(x)$, is modelled as having a quadratic form with an interaction term in latitude and longitude. Letting $m(x)$ and $n(x)$ denote the longitude and latitude of location x respectively, it is assumed that

$$\mu_0(x) = \mu_{0,1} + \mu_{0,2}m(x) + \mu_{0,3}n(x) + \mu_{0,4}m(x)^2 + \mu_{0,5}n(x)^2 + \mu_{0,6}m(x)n(x) \quad \forall x \quad (7)$$

The spatio-temporal dynamic term $\theta(x, t)$ is modelled as a vector autoregressive model of order one, conditionally specified on its nearest neighbours in all cardinal directions, as shown in eq. 8.

$$\begin{aligned} \theta(x, t) = & b_0\theta(x, t-1) + b_N\theta(x^N, t-1) + b_E\theta(x^E, t-1) \\ & + b_S\theta(x^S, t-1) + b_W\theta(x^W, t-1) + \varepsilon_\theta(x, t) \quad \forall x, t \end{aligned} \quad (8)$$

There were no obvious rationale for allowing the grid-point specific autoregressive parameter b_0 to vary spatially, as in [18]. Hence, b_0 as well as the parameters corresponding to the nearest neighbours, b_N, b_E, b_S, b_W are assumed invariant in space. These parameters are assumed to have interpretations connected with the underlying ocean dynamics and how sea states behave and change over an area. Since the various components are specified conditionally, the different noise contributions $\varepsilon_Y(x, t)$, $\varepsilon_\mu(x)$ and $\varepsilon_\theta(x, t)$ should be identifiable, as pointed out by [18].

The seasonal component is modelled as an annual cyclic contribution assumed independent of space, as shown in eq. 9. A noise term is included in this part of the model, as opposed to e.g. the model in [34]. The period of the seasonal cycle is one year, so $\omega = \frac{2\pi}{12}$ for monthly data, $\omega = \frac{2\pi}{365.25}$ for daily data and $\omega = \frac{2\pi}{1461}$ for six-hourly data, taking the average number of observations over normal and leap-years. Apriori, it is known that the worst weather normally occurs around the beginning of the year (January), so d , which represents a temporal shift from a pure cosine cyclic component, is presumably small.

$$M(t) = c \cos(\omega t) + d \sin(\omega t) + \varepsilon_m(t) \quad \forall t \geq 1 \quad (9)$$

The long-term trend is modelled as a simple Gaussian process with a quadratic trend, as shown in eq. 10. Noise terms, assumed independent and identically distributed with zero mean and variance σ_T^2 , are included in this component as well. Presumably, the parameters γ and η will be very small since they correspond to the increase over one month/one day/6 hours due to the long-term trend. However, the trend might be detectable as it accumulates over long periods of time.

$$T(t) = \gamma t + \eta t^2 + \varepsilon_T(t) \quad \forall t \geq 1 \quad (10)$$

3.2 Model alternatives

Different model alternatives were tried and simulations were run for five different model alternatives, i.e. with a quadratic trend, linear trend and no temporal trend respectively and with one or two temporal noise terms as summarized below. For the models with only one temporal noise term, the long-term trend and the seasonal components are combined in a temporal part $M(t)$. All other model components remain unchanged.

- 1: $T(t) = \gamma t + \eta t^2 + \varepsilon_T(t)$
- 2: $T(t) = \gamma t + \varepsilon_T(t)$
- 3: $T(t) = 0$
- 4: $M(t) = c \cos(\omega t) + d \sin(\omega t) + \gamma t + \eta t^2 + \varepsilon_m(t)$
- 5: $M(t) = c \cos(\omega t) + d \sin(\omega t) + \gamma t + \varepsilon_m(t)$

Table 1: Specification of prior distributions

Parameters	Prior distribution
$\sigma_Y^2, \sigma_\mu^2, \sigma_\theta^2, \sigma_m^2$ and σ_T^2	$IG(3, 2)$
$a_\phi, a_\lambda, b_0, b_N, b_E, b_S$ and b_W	$N(0.2, 0.25)$
$\mu_{0,i}$ for $i = 2, \dots, 6$	$N(0, 2)$
$\mu_{0,1}$	$N(3.5, 2)$
$\theta(x, 0)$ for all x	$N(0, 15)$
c	$N(2, 0.5)$
d	$N(0, 0.2)$
γ and η	$N(0, 0.1)$

3.3 Prior distributions on the model parameters

The model outlined in the preceding section will be specified in a Bayesian setting, and the model is completed by specifying prior distributions on the various model parameters. In line with the assumptions made in [18], all prior distributions are assumed independent, and the following model parameters requires specification of a prior distribution: The noise variances $\sigma_Y^2, \sigma_\mu^2, \sigma_\theta^2, \sigma_m^2$ and σ_T^2 , the MRF parameters a_ϕ and a_λ , the spatial mean parameters $\mu_{0,i}$ for $i = 1, \dots, 6$, the vector autoregressive parameters b_0, b_N, b_E, b_S and b_W , the variables of the autoregressive process $\theta(x, 0)$ for $x = 1, \dots, X = 153$, the seasonal parameters c and d and the temporal trend parameters γ and η . Specification of prior distributions for these 175 parameters together with initial values for $\theta(x, 0)$ would thus complete the specification of the model, and for sensible prior distributions the full posterior conditional distributions can be derived. This will be ensured by specifying conditionally conjugate priors for all these parameters.

For the purpose of this study, the same priors as was used in the model for the original data [29] are adopted for all model parameters, and the prior distributions with hyperparameters are specified in Table 1. The model is then fully specified.

4 Loss functions for model comparison and selection

Statistical models are often compared by way of the AIC or BIC criteria presented by [1, 21], but neither are straightforward to use for complex hierarchical models. An alternative criterion proposed for comparing complex hierarchical models is the deviance information criterion (DIC) ([22]). However, neither of these have been employed in the current study, which explores approaches for model comparison and selection by way of loss functions based on short-term predictive power. It is noted that short-term predictive power may not be a good measure for a model aiming at identifying long-term trend so robust model selection remains an open issue. It is also noted that only the observational level is used for model comparison. Hence, the approach is conditional on the underlying system levels.

It would also be desirable to compare the results stemming from the log-transformed model with the results obtained without the log-transform as reported in [29]. In order to facilitate this, the loss functions should be based on prediction errors on the original scale. Thus, the loss functions are based on $Z(x)$ and not $Y(x)$ and should therefore be suited for comparison with the results for the original data. Likelihood approaches and criteria based on sum of squares are not ideally suited for model selection in complex hierarchical models, and will not be used in this study. It is merely noted that the goodness-of-fit seemed to improve with the log-transformation compared to the results reported in [29].

Two loss functions based on predictive power were constructed as alternative ways to compare the models. Only one-step predictions were considered. Hence, the model was fitted with all data except

the last timepoint, and predictions of the spatial field at this timepoint for the various models were then compared to the data. Predictions and data were transformed back to the original scale in doing so.

In the following, the predictions $Z(x)_j^*$ are taken as the estimated value of $Z(x)$ given the samples for all model parameters and variables in iteration j . The model specification gives

$$\mathbf{Z}(x)_j^* = e^{\mu(x)_j + \theta(x,t)_j + M(t)_j + T(t)_j + \varepsilon_Y(x,t)_j} = e^{\mu(x)_j + \mathbf{B}_j \boldsymbol{\theta}(t-1)_j + c_j \cos(\omega t) + d_j \sin(\omega t) + \gamma_j t + \eta_j t^2 + \varepsilon_Z(x)_j} \quad (11)$$

where the subscript j denotes the sampled parameters in iteration j and the noise terms $\varepsilon_Z(x)$ are sampled independently from a zero-mean normal distribution with variance $\sigma_{Z,j}^2 = \sigma_{Y,j}^2 + \sigma_{\theta,j}^2 + \sigma_{m,j}^2 + \sigma_{T,j}^2$. Note that since $\mu(x)$ is independent of time, the sampled values of $\mu(x)_j$ can be used and these have already incorporated the noise term ε_μ . Hence, this noise term is not a part of $\varepsilon_Z(x)$ when making the predictions. \mathbf{B} is an $X \times X$ matrix with the b -parameters as elements as follows

$$b_{kl} = \begin{cases} b_0 & \text{if } k = l \\ b_N & \text{for } l = \text{neighbor to the North of } k \\ b_E & \text{for } l = \text{neighbor to the East of } k \\ b_S & \text{for } l = \text{neighbor to the South of } k \\ b_W & \text{for } l = \text{neighbor to the West of } k \\ 0 & \text{otherwise .} \end{cases} \quad (12)$$

4.1 Standard loss function

Analogue to the standard loss function used in [18], the standard loss function in eq. 13 is defined where $Z(x)$ denotes the data at location x and $Z^*(x)_j$ denotes the predicted value of Z at location x in iteration j .

$$L_s = \left[\frac{1}{Xn} \sum_{x=1}^X \sum_{j=1}^n \left(Z(x) - Z(x)_j^* \right)^2 \right]^{\frac{1}{2}} \quad (13)$$

4.2 Weighted loss function

More specially designed loss functions may also be used, for example where a greater penalty is introduced for failing to predict an extreme sea state compared to prediction errors for less severe sea states or where the spatial predicted fields are smoothed by averaging over neighboring gridpoints (as in [18]). In this study, one alternative loss function has been designed, where the squared prediction errors have been weighted according to the actual observed significant wave height. More precisely, a weight of $Z(x)$ is included in order to give greater emphasis on prediction errors at locations where large significant wave heights have been observed. Hence, an alternative loss function as given in eq. 14 is calculated.

$$L_w = \left[\frac{1}{n \sum_x Z(x)} \sum_{x=1}^X \sum_{j=1}^n Z(x) \left(Z(x) - Z(x)_j^* \right)^2 \right]^{\frac{1}{2}} \quad (14)$$

5 Markov Chain Monte Carlo simulations

In order to simulate the model, MCMC techniques (Gibbs sampling with Metropolis-Hastings steps, see e.g. [20]) have been employed. This requires the full conditional distributions for all the parameters involved, which is completely determined by the model and the prior distribution specifications. Gaussian distributions and conjugate priors have been used, so the derivation of the full conditional distributions have been rather straightforward in most cases. The derivation of the full conditionals follow the same lines as for the

non-transformed model and will not be repeated herein, but reference is made to the appendix of [29] for details.

45,000 iterations were run for the monthly data, with an initial burn-in period of 20,000 and then keeping every 25th sample (batch size = 25). For the daily and six-hourly data, when simulations became increasingly time consuming, the batch size was reduced to 5, retaining the burn-in period of 20,000. Thus, a total of 1000 samples of the multi-dimensional parameter vector were obtained from each simulation. A set of simulations were also run for the monthly data with a batch size of 5, and this produced nearly identical results, but with slightly wider credibility bands. This can be explained by the greater Monte Carlo variance for samples that are more correlated, and is as expected. In addition, goodness of fit and short-term predictions are minimally affected. Notwithstanding, for daily and six-hourly simulations, which are much more time consuming, a batch size of 5 was used.

No formal tests on convergence have been carried out, but visual inspection indicates that convergence occurs relatively quickly. A few simulations have been performed with different starting values for the parameter set and the results indicate that the Gibbs sampler has indeed converged. In addition, control simulations with considerably longer burn-in periods were run for the monthly data, and these showed nearly identical results, indicating that convergence did indeed occur within the burn-in period. However, it cannot be taken for granted that convergence occur equally fast for daily and six-hourly data.

6 Simulation results and predictions

6.1 Results for monthly data

In order to check the Gaussian model assumption in eq. 2 for the log-transformed data, a visual check of the residuals was carried out. It is observed that the normal probability plot in figure 4 (for the quadratic model) looks much better than the corresponding plot for non-transformed data [29]. This indicates that the log-transform may represent an improvement. However, there still seems to be some spatial dependence in the residuals, but this is presumably due to edge-effects, i.e. where there are no neighbor in one direction. The same features were also observed for the non-transformed data. Nevertheless, the QQ-plot shows that the model indeed performs well.

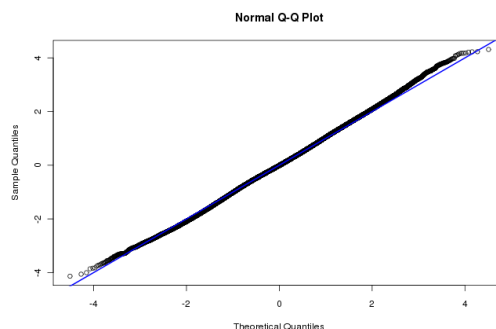


Figure 4: Normal probability plot of the residuals, monthly data

Most of the marginal posterior distributions are close to Gaussian, and the mean and standard deviation of the posterior distributions for different parameters of the different model alternatives are given in table 2. It is seen that apart from the temporal trend part, most of the model parameters do not vary significantly between model alternatives. It is emphasized that these parameters pertain to the log-transformed data, and the values are therefore not comparable to the values obtained for the non-transformed data. However,

Table 2: Posterior marginal distributions, mean and standard deviation; monthly log-transformed data

	Model 1	Model 2	Model 3	Model 4	Model 5
σ_z^2	(0.057, 0.00034)	(0.057, 0.00036)	(0.057, 0.00034)	(0.057, 0.00036)	(0.057, 0.00036)
σ_μ^2	(0.027, 0.0030)	(0.027, 0.0030)	(0.027, 0.0030)	(0.027, 0.0032)	(0.027, 0.0030)
σ_θ^2	(0.0079, 0.00021)	(0.0079, 0.00021)	(0.0079, 0.00022)	(0.0079, 0.00020)	(0.0079, 0.00020)
σ_m^2	(0.063, 0.0065)	(0.061, 0.0068)	(0.10, 0.0061)	(0.10, 0.0062)	(0.10, 0.0061)
b_0	(0.21, 0.0079)	(0.21, 0.0078)	(0.21, 0.0076)	(0.21, 0.0079)	(0.21, 0.0081)
b_N	(0.17, 0.0091)	(0.17, 0.0094)	(0.17, 0.0094)	(0.17, 0.0090)	(0.17, 0.0093)
b_E	(0.21, 0.0087)	(0.21, 0.0087)	(0.21, 0.0084)	(0.21, 0.0086)	(0.21, 0.0086)
b_S	(0.16, 0.0092)	(0.16, 0.0090)	(0.16, 0.0094)	(0.16, 0.0094)	(0.16, 0.0099)
b_W	(0.19, 0.0081)	(0.19, 0.0079)	(0.19, 0.0078)	(0.19, 0.0084)	(0.19, 0.0079)
c	(0.35, 0.022)	(0.35, 0.021)	(0.35, 0.019)	(0.35, 0.020)	(0.35, 0.019)
d	(0.26, 0.021)	(0.26, 0.021)	(0.26, 0.019)	(0.26, 0.020)	(0.26, 0.019)
$\mu_{0,1}$	(3.5, 1.4)	(3.4, 1.4)	(3.5, 1.4)	(3.4, 1.5)	(3.5, 1.4)
$\mu_{0,2}$	(-0.089, 0.038)	(-0.087, 0.037)	(-0.089, 0.038)	(-0.089, 0.039)	(-0.087, 0.037)
$\mu_{0,3}$	(0.43, 0.22)	(0.43, 0.22)	(0.44, 0.22)	(0.44, 0.22)	(0.42, 0.22)
$\mu_{0,4}$	(0.00016, 9.5×10^{-5})	(0.00016, 9.5×10^{-5})	(0.00016, 9.4×10^{-5})	(0.00016, 9.6×10^{-5})	(0.00016, 9.5×10^{-5})
$\mu_{0,5}$	(-0.0027, 0.0012)	(-0.0026, 0.0011)	(-0.0026, 0.0012)	(-0.0027, 0.0012)	(-0.0026, 0.0012)
$\mu_{0,6}$	(-0.00037, 0.00054)	(-0.00035, 0.00054)	(-0.00038, 0.00052)	(-0.00037, 0.00052)	(-0.00036, 0.00054)
a_ϕ	(0.083, 0.074, 0.058)	(0.083, 0.074, 0.056)	(0.086, 0.077, 0.058)	(0.086, 0.080, 0.056)	(0.086, 0.075, 0.059)
a_λ	(0.087, 0.079, 0.058)	(0.085, 0.076, 0.057)	(0.086, 0.080, 0.056)	(0.088, 0.080, 0.058)	(0.085, 0.079, 0.055)
σ_t^2	(0.059, 0.0064)	(0.062, 0.0070)	-	-	-
γ	(0.00039, 0.00039)	(0.00019, 9.8×10^{-5})	-	(5.9×10^{-5} , 0.00042)	(0.00016, 8.0×10^{-5})
η	(-4.0×10^{-7} , 7.3×10^{-7})	-	-	(1.1×10^{-7} , 7.4×10^{-7})	-

dependence parameters in space and time are presumably similar. In particular, the observational variance does now correspond to a multiplicative noise term for the significant wave height rather than an additive one. The posterior distributions for a_ϕ and a_λ are not Gaussian, so the posterior distributions for these are presented in table 2 in terms of the triplets (mean, median, standard deviation).

A control run with longer burn-in period and longer batch size was performed, i.e. a burn-in of 200,000 and a batch size of 50. This produced nearly identical results and hence illustrates that the burn-in of 20,000 and the batch size of 25 were sufficient. Hence, at least for the monthly data, convergence of the Markov chain is not an issue. The control run was performed for the linear model with two temporal noise terms (model alternative 2).

The six parameters μ_0 , determine the spatially varying mean $\mu_0(x)$ over the area, and gives a similar picture as for the non-transformed data, but with different values. Also the time independent part $\mu(x)$ looks reasonable; figure 5 displays both the mean of $\mu(x)$ (left) and the mean deviation from the mean $\mu(x) - \mu_0(x)$ (right). The contribution from the time-independent part $\mu(x)$ is seen to be in the order of 0.83 - 1.1 but the interpretation is now different. $e^{\mu(x)}$ is a multiplicative factor for the significant wave height at location x varying between 2.3 and 2.9. Again, the mean deviation from the spatially varying mean is rather small, and the range of deviations are from -0.082 to 0.035 (this refers to the model with quadratic trend and two temporal noise terms, but very similar results were obtained for the other model alternatives). In the following, all figures unless stated otherwise are all from simulations over the main model (model 1), but the alternative models give very similar results.

It is somewhat more difficult to visualize the space-time dynamic part, $\theta(x, t)$, since this varies for each time-point. Figure 6 shows the mean and variance of the $\theta(x)$ field for an arbitrary time. For all times (except $t=0$) and locations, the mean ranges from -0.26 to 0.40 with variances ranging from 0.0062 to 0.054. Again, for the log-transformed data, $\theta(x, t)$ corresponds to a multiplicative factor of the significant wave height at time-point (x, t) and the estimated mean values corresponds to factors between 0.77 to 1.5. The average corresponds to a factor of 1 as it should. Hence, a noticeable part of the modelled significant wave

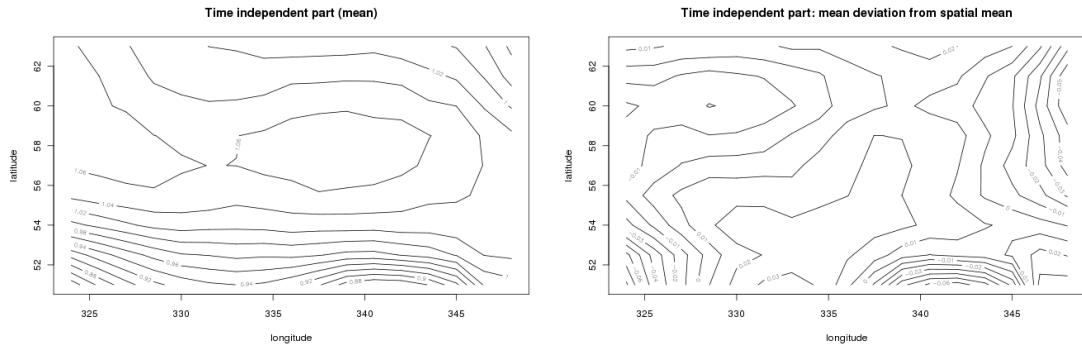


Figure 5: Mean time-independent part varying between 2.3 and 2.9 (left) and deviation from the spatial mean (right), monthly data

height can be ascribed to this space-time dynamic part. It is interesting to note that, of the b -parameters except b_0 , b_E is the largest. This should mean that the model suggests that more storms arrive from East than from the other directions, which is counter-intuitive. However, it is noted that this component is not very meaningful when using monthly data, and a better interpretation will be obtained when running on daily or 6-hourly data. In that case, it is expected that the model should correctly capture the direction most storm tracks follow in the area.

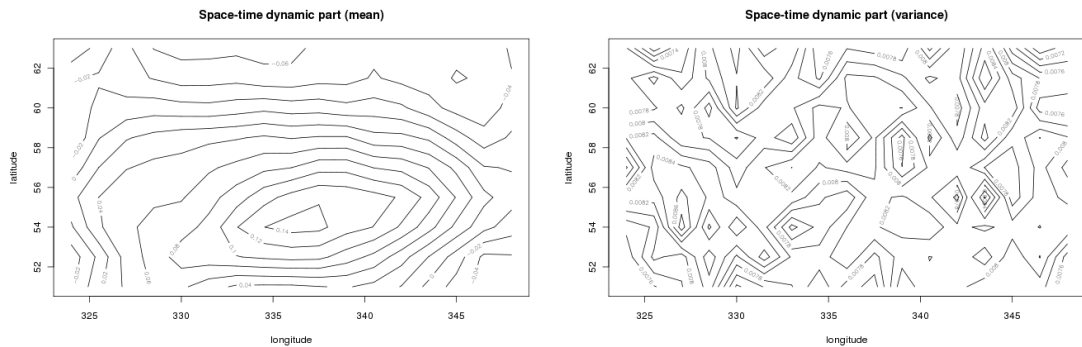


Figure 6: Mean and variance of the dynamic part, corresponding to factors between 0.77 to 1.5, monthly data

The seasonal term for the first ten years is shown in figure 7, and a clear cyclic behaviour is observed. The expected seasonal contribution without the error term, $c \cos(\omega t) + d \sin(\omega t)$ calculated with the mean values of c and d , is also shown in the figure and agrees well with the sampled seasonal contribution. Again, for the log-transformed data, this component corresponds to a multiplicative constant. The expected seasonal component varies cyclically between ± 0.43 , corresponding to a seasonal factor of 0.65 for quiet seasons and 1.5 in rough seasons. For example, for a mean of 3 meters, this corresponds to variations between 2.0 and 4.6 meters due to seasonal effects. Again, these seem reasonable and is comparable to the seasonal component for the non-transformed data.

The temporal trend part of model alternatives 1 and 2 are illustrated in figure 8. The figure shows the sampled mean annual trend together with the mean, 5- and 95-percentiles of the trend contribution obtained by calculating $\gamma t + \eta t^2$ using the corresponding quantiles of the joint distribution of (γ, η) . A horizontal line

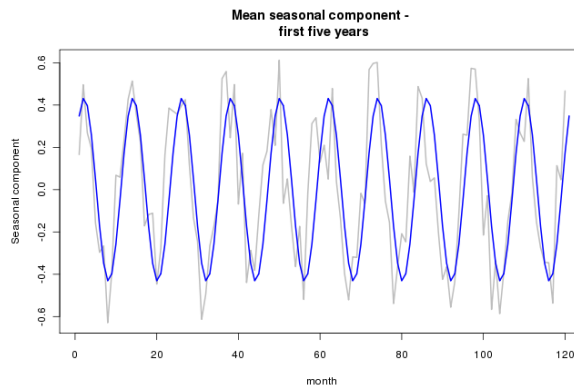


Figure 7: The seasonal component for ten years, monthly data

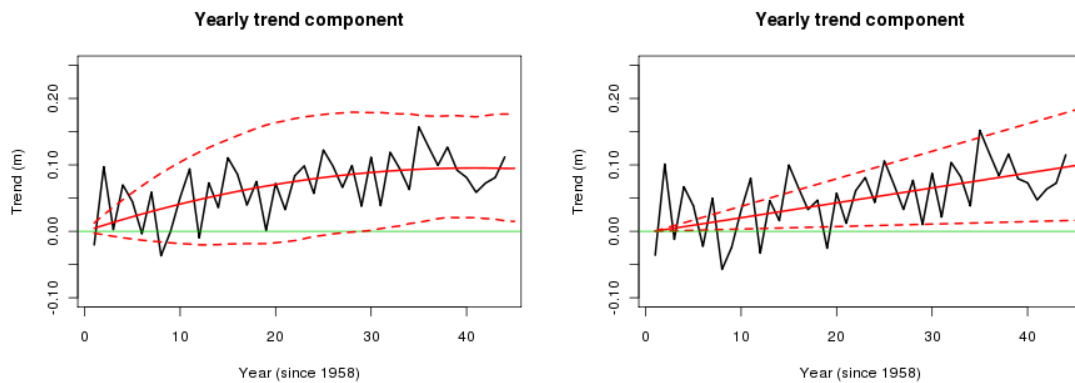


Figure 8: Annual trend over the period, model 1 (left) and model 2 (right), monthly data

corresponding to no trend is also included in the figures. The mean yearly trend according to the quadratic model (model 1) corresponds to a noticeable increase in significant wave height, by a factor of about 1.1 over the period. The 90% credible interval ranges from a factor of 1.01 to 1.19. It is observed that for a mean significant wave height of 3 meters, this expected increase corresponds to an increase of 30 cm. However, for extremes, say above 10 meters, such a multiplicative trend would correspond to an increase of over 1 m over the period.

The linear model (model alternative 2) estimates a mean long-term trend corresponding to an increase in significant wave height of about 10% over the whole period. The 90% credible interval corresponds to an increasing trend between 1.7% and 20%. For an average sea state with significant wave height 3 meters, such an increase would correspond to an expected increase of about 31 cm. For extremes, say above 10 meters, this increase would correspond to an expected increase in significant waveheight of about 1.0 meter. For the mean sea states, these estimates correspond reasonably well with the estimates of the trend obtained from the non-transformed data. However, with a multiplicative trend rather than an additive one, the increase in the extremes will be greater than the increase in average and less extreme sea states.

For the models with one temporal noise term, the seasonal and trend components were not sampled individually, but the estimated trend components are illustrated in figure 9. The long-term trend estimated from these models are comparable to the ones estimated with two noise terms. The quadratic trend model

Table 3: Values of the loss functions, monthly data

Model alternative	L_s	L_w
Model 1	3.4119453	3.5604366
Model 2	3.4247630	3.5459232
Model 3	3.2667590	3.4683411
Model 4	3.3168082	3.4679681
Model 5	3.2979152	3.454546

(Model 4) estimates a mean increase over the period of about 6.3%, but with the 90% credible interval ranging from a decreasing trend of -2% to 15% increase. For sea states of 3 and 10 meters significant wave height, such increases correspond to expected increases of 19 and 63 cm respectively, somewhat less than what was estimated by the model with one temporal noise term. 90% credible intervals would range from -6 - 46 cm and -20 - 153 cm respectively. The linear trend model (Model 5) estimates a mean increase of 8.8% during the period, with a 90% purely increasing credible interval ranging from 1 to 17%. Corresponding expected increase for moderate ($H_s = 3$ m) and rough ($H_s = 10$ m) sea states are 26 and 88 cm respectively, with 90% credible intervals ranging from 4 to 51 cm and 14 to 170 cm respectively.

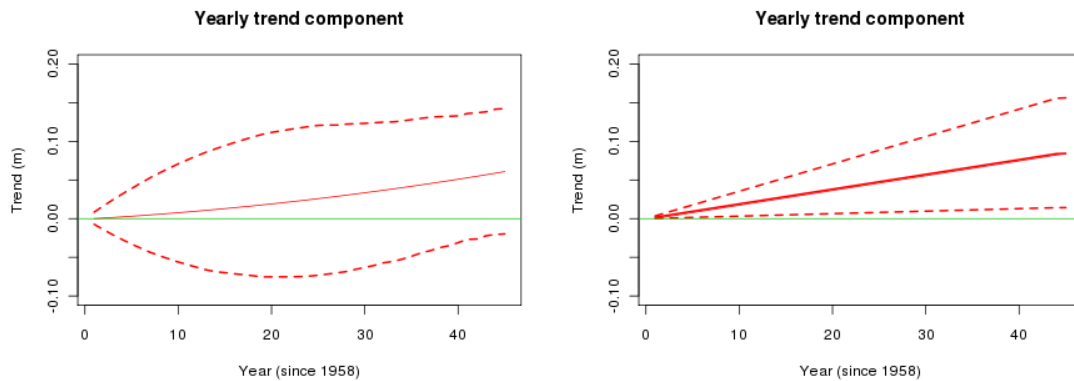


Figure 9: Estimated trend contribution from model 4 (left) and model 5 (right), monthly data

6.1.1 Model comparison and selection

The different model alternatives can generally be compared by comparing the resulting posterior estimates of the model parameters, as presented in table 2. From these tables, it is observed that the parameters related to the spatial features of the model seem to be little affected by the model reductions. Keeping in mind that the model reductions were only related to the temporal trend, it is reassuring to observe that all model alternatives give similar estimates for the spatial parts of the model. Also, the seasonal part of the model seems to behave rather similarly for the different model alternatives. Hence, the main differences are, as would be expected, related to the long term temporal trend parameters γ and η .

The two loss functions, which compared the model predictions with the data for the final time-point, T , were also estimated for the various model alternatives. These were referred to as the standard loss function and the weighted loss function respectively, given by 13 and 14. The values for the two loss functions for the respective model alternatives are included in Table 3. It is noted that no reward is given here for parsimony,

and only predictive power is included in the loss functions. According to the standard loss function, the model with no trend is better and according to the weighted loss function, the model with linear trend and one temporal noise term is rendered better. It is also interesting to note that, in spite the fact that the model for log-transformed data yields better goodness-of-fit compared to the original data, the models for the original data seem to perform consistently better with regards to short-term prediction. Notwithstanding, it is difficult to assess the models in terms of long-term prediction and it is still an open question which model alternative would be better in this regard.

6.2 Results for daily data

The same model was also run for daily data, i.e. using one observation per day. Running these simulations were much more computational intensive than the monthly data, but less so than the full dataset of six-hourly observations; one set of simulations, now with a burn-in-period of 20,000 but with a batch size of 5 completed in about 200 hours. The model was run with the same five model alternatives as described above, and the results from these simulations are summarized below.

The normal probability plot of the residuals in figure 10 (for the quadratic model) looks better than the corresponding plot for non-transformed data, suggesting that the model assumptions are reasonable. Again, most of the marginal distributions resemble Gaussian distributions, and the mean and standard deviation of the posterior distributions for the various parameters are given in table 4 (mean, median and standard deviation for a_ϕ and a_λ). It is observed that apart from the temporal trend part, most of the model parameters do not vary significantly between model alternatives.

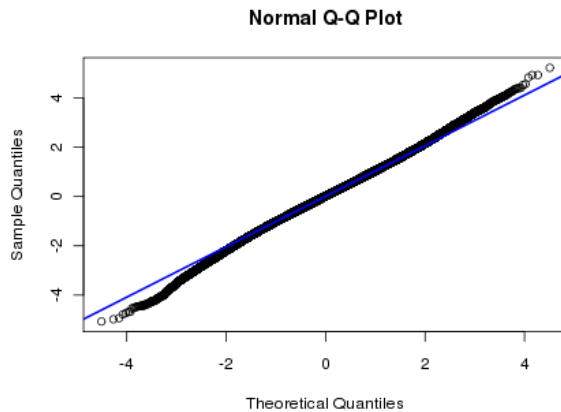


Figure 10: Normal probability plot of the residuals, daily data

The figures displaying these results are very similar to the ones for monthly data and will not be presented, but the main results are summarized briefly in the following. The contribution from the time-independent component, $\mu(x)$, is now a factor between 0.89 - 1.2, corresponding to a multiplicative factor varying between 2.4 and 3.2 for different locations, x . This is slightly higher than the factors obtained with monthly data, but within the same order of magnitude. The deviations from the spatially varying means are again small.

The contribution from the space-time dynamic component, $\theta(x, t)$, has now become more significant with the mean ranging from -0.91 to 0.75 and variances between 0.0089 to 0.038, corresponding to multiplicative factors between 0.40 and 2.1. This corresponds to a ratio of 5.25 between significant wave heights during storms and quiet periods. The corresponding ratio obtained with monthly data was less than 2. Now, b_W is the largest of the b -parameters, except b_0 , and this is reassuring. It indicates that the model is now able to capture the main storm tracks, which are known to be predominantly from West to East in this

Table 4: Posterior marginal distributions, daily log-transformed data

	Model 1	Model 2	Model 3	Model 4	Model 5
σ_z^2	(0.035, 5.5×10^{-5})	(0.035, 5.3×10^{-5})	(0.035, 5.8×10^{-5})	(0.035, 5.5×10^{-5})	(0.035, 5.6×10^{-5})
σ_μ^2	(0.027, 0.0031)	(0.027, 0.0030)	(0.027, 0.0030)	(0.027, 0.0032)	(0.027, 0.0030)
σ_θ^2	(0.016, 4.8×10^{-5})	(0.016, 4.6×10^{-5})	(0.016, 4.9×10^{-5})	(0.016, 4.7×10^{-5})	(0.016, 4.7×10^{-5})
σ_m^2	(0.040, 0.00090)	(0.040, 0.0013)	(0.082, 0.00095)	(0.081, 0.00092)	(0.082, 0.00093)
b_0	(0.24, 0.0011)	(0.24, 0.0012)	(0.24, 0.0011)	(0.24, 0.0012)	(0.24, 0.0011)
b_N	(0.12, 0.0011)	(0.12, 0.0010)	(0.12, 0.0011)	(0.12, 0.0011)	(0.12, 0.0010)
b_E	(0.13, 0.0011)	(0.13, 0.0011)	(0.13, 0.0011)	(0.13, 0.0012)	(0.13, 0.0011)
b_S	(0.16, 0.0011)	(0.16, 0.0011)	(0.16, 0.0011)	(0.16, 0.0011)	(0.16, 0.0011)
b_W	(0.28, 0.0012)	(0.28, 0.0011)	(0.28, 0.0012)	(0.28, 0.0012)	(0.28, 0.0011)
c	(0.45, 0.0034)	(0.45, 0.0035)	(0.45, 0.0032)	(0.45, 0.0032)	(0.45, 0.0033)
d	(0.097, 0.0035)	(0.096, 0.0034)	(0.096, 0.0033)	(0.097, 0.0032)	(0.097, 0.0033)
$\mu_{0,1}$	(3.4, 1.4)	(3.5, 1.4)	(3.5, 1.4)	(3.4, 1.4)	(3.4, 1.4)
$\mu_{0,2}$	(-0.091, 0.037)	(-0.086, 0.038)	(-0.088, 0.036)	(-0.089, 0.038)	(-0.089, 0.038)
$\mu_{0,3}$	(0.45, 0.21)	(0.42, 0.22)	(0.44, 0.20)	(0.44, 0.22)	(0.44, 0.22)
$\mu_{0,4}$	(0.00017, 9.1×10^{-5})	(0.00016, 9.6×10^{-5})	(0.00017, 9.1×10^{-5})	(0.00017, 9.6×10^{-5})	(0.00017, 9.6×10^{-5})
$\mu_{0,5}$	(-0.0026, 0.0012)	(-0.0024, 0.0012)	(-0.0025, 0.0011)	(-0.0025, 0.0012)	(-0.0025, 0.0012)
$\mu_{0,6}$	(-0.00045, 0.00049)	(-0.00042, 0.00053)	(-0.00043, 0.00051)	(-0.00043, 0.00053)	(-0.00044, 0.00053)
a_ϕ	(0.085, 0.078, 0.055)	(0.085, 0.076, 0.057)	(0.086, 0.080, 0.055)	(0.087, 0.079, 0.056)	(0.085, 0.077, 0.057)
a_λ	(0.086, 0.077, 0.056)	(0.084, 0.076, 0.056)	(0.089, 0.081, 0.060)	(0.088, 0.080, 0.057)	(0.086, 0.078, 0.058)
σ_t^2	(0.043, 0.0011)	(0.042, 0.0013)	-	-	-
γ	(-5.6×10^{-7} , 1.3×10^{-6})	(4.3×10^{-6} , 3.1×10^{-7})	-	(-7.0×10^{-6} , 1.3×10^{-6})	(3.9×10^{-6} , 4.3×10^{-7})
η	(3.0×10^{-10} , 8.7×10^{-11})	-	-	(6.4×10^{-10} , 9.0×10^{-11})	-

particular area. It is not surprising, however, that this was not well captured when using monthly data, since no storms endure for that long. At any rate, it is reassuring to observe that this component behaves as it should for temporal resolutions comparable to duration of storms, and this component now has a more meaningful interpretation.

The seasonal component for the first five years is shown in figure 11. The expected seasonal component varies cyclically between ± 0.46 , corresponding to a seasonal factor of 0.63 for quiet seasons and 1.6 in rough seasons. For example, for a mean of 3 meters, this corresponds to variations between 1.9 and 4.8 meters due to seasonal effects, and this is comparable to the seasonal effect obtained for the non-transformed data in [29].

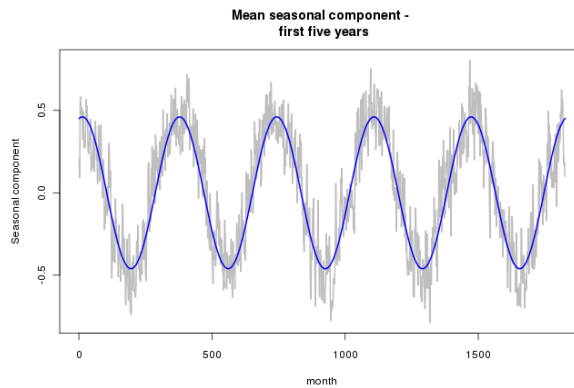


Figure 11: The seasonal component for five years, daily data

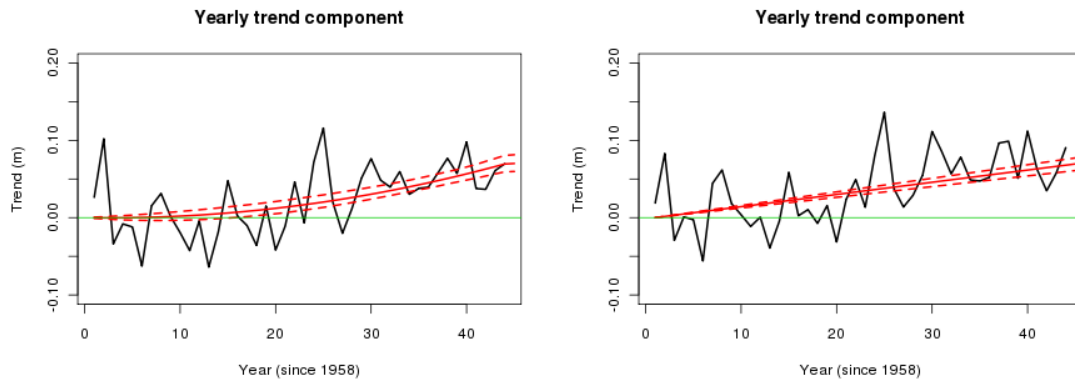


Figure 12: Annual trend over the period, model 1 (left) and model 2 (right), daily data

The temporal trend part of the quadratic and linear models (models 1 and 2) are illustrated in figure 12. A significant positive trend can be extracted from the data and yearly trends corresponding to a noticeable increase in significant wave height is observed. The quadratic model (model 1) estimates a mean factor of about 1.07 over the period. The 90% credible interval ranges from a factor 1.06 to a factor about 1.08. It is observed that for a mean significant wave height of 3 meters, this expected increase corresponds to an increase of 22 cm. However, for extremes above 10 meters, such a multiplicative trend would correspond to an increase of over 73 cm over the period. The corresponding 90% credible intervals are 18 to 25 cm and 62 to 85 cm respectively.

The mean estimate of the long-term trend from the linear model corresponds to an increase of about 7.2% over the whole period. The 90% credible interval ranges from 6.3 to 8.1%. For an average seastate with significant wave height 3 meters, such an increase would correspond to an expected increase of 22 cm, but with an increase of at least 19 cm. For extremes above 10 meters, this would correspond to an expected increase in significant wave height of 72 cm and with 95% credibility, at least 63 cm. It is noted that these trend estimates are somewhat lower than what was extracted from the monthly data, but with much narrower credibility bands.

For the models with a single temporal noise term, the seasonal and trend components were not sampled individually, but the estimated trend components are shown in figure 13. The quadratic trend model (Model 4) estimates a mean increase over the period of about 5.5%, but with the 90% credible interval ranging from 4.3 to 6.7%. This corresponds to expected increases of 16 and 55 cm for moderate and rough sea states respectively. Corresponding 90% credible intervals range from 13 to 20 cm and 43 to 67 cm respectively. The linear trend model (Model 5) estimates a mean increase of 6.5% during the period, with a 90% credible interval ranging from 5.2 to 7.6%. Corresponding expected increases for moderate and rough sea states are 19 and 65 cm respectively, with 90% credible intervals ranging from 16 to 23 cm and 52 to 76 cm respectively. It is noted that these trends are slightly less than the trends estimated with two temporal noise terms, but they are within the same order of magnitude and there is general agreement among the models that there are a significant increasing trend in significant wave height.

6.2.1 Model comparison and selection

Comparing the estimated posterior distributions for the model parameters in table 4, it is again observed that most model parameters, except those related to the trend components, remain unaffected by the changes of models. The loss functions associated with the prediction error for the final time-point for the different model alternatives are given in table 5. Both loss functions favor the quadratic models, and the models with

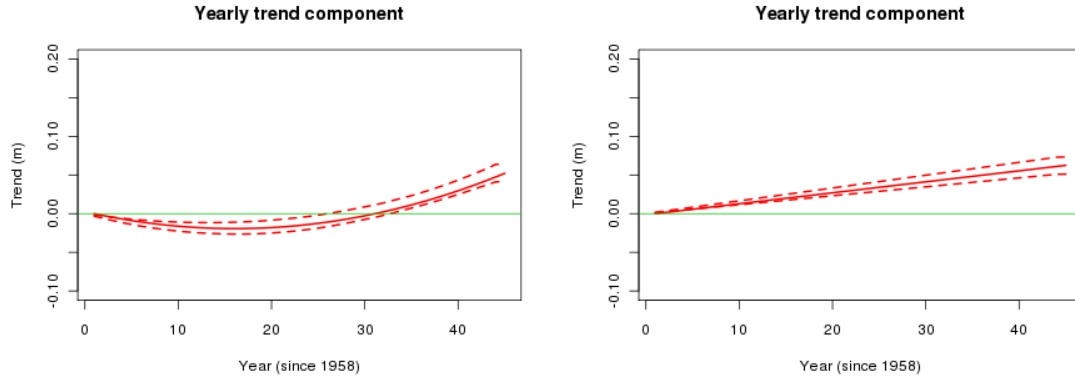


Figure 13: Estimated long term trend contribution for model 4 (left) and model 5 (right), daily data

Table 5: Values of the loss functions, daily data

Model alternative	L_s	L_w
Model 1	2.5615432	2.6654849
Model 2	2.5729260	2.6842552
Model 3	2.6002640	2.7280551
Model 4	2.5569820	2.6550046
Model 5	2.5692487	2.6816735

a single temporal noise terms have slightly smaller values for the loss functions.

6.3 Simulations on 6-hourly data

The same model was also run for the full data-set, exploiting the full six-hourly resolution. Running these simulations were very computational intensive with more than one month in pure computing time for each set of simulations (each simulation required about 6000 CPU-hours). The burn-in-period was still 20,000 and with a batch size of 5. The model was run with the same five model alternatives as described above, but there were some indications of lack of convergence of the Markov chain, at least for some of the model alternatives.

Traceplots of the estimated trend contribution at time $t = T$, for example, displays a discernable increasing drift for the models with two temporal noise terms. In comparison, the traceplots from the model with only a single temporal noise term looks more stationary without any notable drift (figure 14). Even though the drift is small, it indicates non-stationarity of the chain, and it is not possible to know at what level the drift would disappear. It appears that the model with one temporal noise term is stationary and it should not be surprising if these models indeed converge faster. Since it cannot be assured that the simulated samples are in fact sampled from the stationary distribution, less confidence is put on the results for the 6-hourly data. Nevertheless, a brief qualitatively description of the simulations will be given below.

The contribution from the purely spatial part of the model remains hardly unchanged by the change in temporal resolution, and this is reassuring. The space-time dynamic component $\theta(x, t)$, however, becomes significantly larger when using 6-hourly data whereas the long-term trend components have become significantly smaller, with narrower credibility bands. It is indeed expected that the short-term dynamic part becomes more important for data with higher resolution, but it is stressed that the chain might not yet have

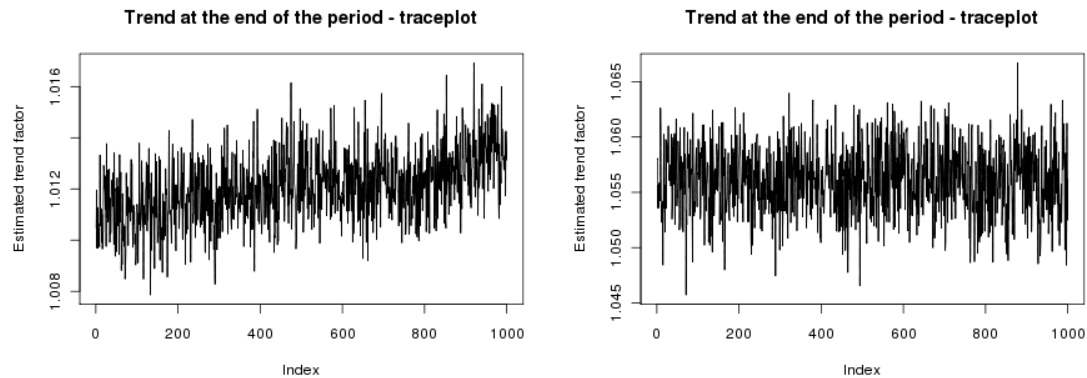


Figure 14: Traceplots for the trend contribution at $t = T$ for the quadratic models with two (left) and one (right) noise terms

converged, and it is possible that it would take time to distinguish between short-term dynamic effects and a long-term trend. The b -parameters again suggest that storms arrive predominantly from the West, and to some extent from the North, but now b_E takes a negative posterior mean, which would mean that significant wave height at a location is negatively correlated to the significant wave height at a location 1.5° to the East, 6 hours before.

The same problems were encountered for the non-transformed data [29] but due to the extremely time-consuming computations, it is unpractical to repeat the simulations with longer burn-in in order to check if the chain then converges³.

6.4 Future projections

Even though extrapolation beyond the time interval for which the models are fitted might not be valid, it is tempting to extend the estimated trends into the future. It is acknowledged that this might be highly speculative. Notwithstanding, assuming that such trends as the ones predicted from the linear models will continue into the future, the corresponding expected increases over 100 years is summarized below. Extrapolation of the quadratic trend functions are deemed even more speculative and will not be performed herein.

6.4.1 Projections based on monthly data

Assuming that a trend such as the one predicted from the linear trend model with two temporal noise terms fitted to monthly data will continue into the future, this would correspond to an expected increase in significant wave height of 25% over 100 years, with a 95% credibility of an increasing trend larger than 3.8%. The corresponding expected increase of 21% with 95% credibility of an increase of at least 3% is obtained from the linear trend model with one temporal noise term for monthly data. Assuming such trends to be valid for all sea states, an expected increase of a sea state of 3 m would then be about 0.75 m (model 2) or 0.63 m (model 4) and for an extreme sea state of 10 m the expected increase would be 2.5 m (model 2) or 2.1 m (model 4) over 100 years. It is noted that the trends for moderate sea states are comparable to the ones obtained from the original data [29], but due to the multiplicative nature of the trends obtained with the log-transform, a much larger trend is now estimated for extremes.

³A couple of simulations were run for the original data with twice as long burn-in period, but it could still not be assured that the chain had converged

6.4.2 Projections based on daily data

If trends such as the ones predicted from the linear trend models fitted to daily data will continue into the future, this would correspond to an expected increase in significant wave height of 17%, with a 95% credibility of an increase of at least 15 % over 100 years for the model with two temporal noise terms (model 2) and an expected increase of 15% with 95% credibility of an increase of at least 12 % for the model with one temporal noise term (model 4). Assuming such trends to be valid for any sea states, the expected increase of a sea state of 3 m would be about 0.50 m or 0.45 m for the two model alternatives and for extreme sea states of 10 m the expected increase would be 1.7 m and 1.5 m over 100 years respectively. Again, it is seen that the expected trend for moderate sea states coincide with the ones estimated with the original data reported in [29], whereas extremes are now assigned a much larger trend.

6.5 Overall comments

Different model alternatives have been tried out and the number of temporal noise terms have been varied between one and two. It is noted that including a second temporal noise term might lead to difficulties in distinguishing between the noise contributions, and simulations for 6-hourly data indicate that the models with an additional temporal noise term need longer time to converge. However, this does not seem to influence the overall results much as long as the stationary distributions are sampled from and the results from either models are similar. Furthermore, even though there might be some identifiability issues for the two temporal noise terms, the added temporal noise seems to be rather constant (see [29]). The models for log-transformed also displayed some border-effects of the spatial fields, similar to those reported in [29].

It is observed that data with higher temporal resolution tend to yield lower estimates for the long-term trend, but with much narrower credibility bands. On the other hand, the short-term, space-time dynamic contributions seem to be increasingly important for higher temporal resolutions. This is as expected, but it is noted that the model might have trouble isolating the long-term trend and that it is possible that the short-term dynamic part, as it becomes increasingly important, partly incorporates and camouflages some long-term trends present in the data. Notwithstanding, comparing the different estimates they all seem to agree fairly well. In particular, all simulations suggest that there is indeed a significant positive trend present in the significant wave height data.

7 Discussion

The results presented above are from the outlined model fitted to log-transformed data. Similar models have also been run for the original data, as reported in [29]. Even though results cannot easily be compared directly between the original and the log-transformed data, the loss functions have used the same scale and these suggest that the models for the original data perform best with regards to short-term prediction. However, goodness-of-fit seem to improve with the log-transform. This could be explained by the observed heteroscedasticity in the original time-series which the model seem to be unable to capture satisfactory, but after the log-transform, the data seem to be homoscedastic.

Another observation is that the models with the log-transformed data seem to be able to estimate the extremes better. In the monthly data set, the maximum significant wave height was 13.24 meters, an extreme significant wave height above 10 meter was recorded 179 times and the minimum value was 0.628 meters. The maximum estimated H_s values were in the range 10 - 10.5 meters for the various models for the original data, and in the range of 13 - 14 meters for the log-transformed data. This suggests that the model for the original data seems to be unable to reproduce the extremes well. Furthermore, with the original data, an extreme value above 10 meter was estimated on average about 1.1 times each iteration, whereas with the log-transformed data this number was increased to about 18 times per iteration. This indicates that

both models seem to underestimate the frequency of extreme sea states, but much less so with the log-transformed data. Comparing the minimum estimated values with the minimum in the data, it is seen that with the original data, minima are estimated about 168 times more frequent than they occur in the data, but that using the log-transformed data leads to too few minima. Finally, a potential problem with using the original data is that, occasionally, one may get an estimated significant wave height less than 0, which is of course unphysical. However, the results indicate that this is not a big issue, with about 0.001% of the estimates having negative H_s values. Nevertheless, this is never a problem if using the log-transformed data.

For the daily data set, the maximum significant wave height was 17.1 meters, extreme significant wave heights above 10 meter were recorded 10,770 times and the minimum value was 0.423 meters. The maximum estimated H_s values were in the range 13 - 14 meters for the various models for the original data, and in the order of 20 meters for the log-transformed data. Hence, again the model for the original data seem to be unable to reproduce the extremes well whereas, for the models with the log-transformed data, extremes might be slightly overestimated. Furthermore, with the original data, extreme values were estimated on average about 2,400 times for each iteration, whereas with the log-transformed data this number was increased to about 4,600 times per iteration. Thus both models seem to underestimate the frequency of extreme sea states, but less so with the log-transformed data. With the original data, minima are estimated much more frequent than they occur in the data, but using the log-transformed data minima are slightly less frequent than in the actual data. Using the original daily data about 0.01% of the estimates gets negative H_s values.

Regarding the different long-term trend components, it is acknowledged that the simple selection criteria employed are not really able to distinguish between them; they all seem to describe the data similarly well. However, if the estimated trends should be used for future predictions, it is assumed that the quadratic trend cannot be extrapolated into the future, and estimates of future trends could only be based on the linear trend. Even this might not be valid, but assuming that one might make such projections, the models predict an expected increase of significant wave height around 45 - 75 cm for moderate sea states and 1.5 - 2.5 meters for extreme sea states over a period of 100 years. The trends for moderate sea states are comparable to the estimated trends obtained without the logarithmic transform of the data, but the estimated trends in the extremes are now much larger than the trends in the mean condition. This feature was also reported by e.g. [36].

It is noted that the future projections estimated from the models seem to be in reasonable agreement to other projections made for significant wave height in the North Atlantic, reported by e.g. [30, 14, 31, 9]. However, it is noted that even though the models seem to detect trends in the data, it does not necessarily mean that the trend is related to climate change. It might be a result of decadal natural variability, as discussed in e.g. [6]. Great care should therefore be taken when interpreting the meaning and the origin of this trend. Furthermore, if the model presented herein should be used for projections and long-term predictions, it is believed that the models need to be extended with appropriate covariates, as briefly discussed below.

Different attempts at model comparison and selection have been suggested in this paper, but neither of them might be ideally suited for such a complex model as this one. In particular, if the aim is to estimate long term temporal trends and to extrapolate those into the future, short-term predictive power might not be a suitable measure of success. In fact, according to the model selection approaches employed, simulations on monthly data seem to favor linear or no trends, daily data quadratic trends and 6-hourly data linear or no trends. This inconsistency is troublesome, but it might just be that this indicates that estimation of such a comparably small trend, distinguishing a genuine trend which is insignificant compared to the other contributions, from the noise, is difficult. It may also illustrate the sensitivity of such models on the temporal resolution of the data. At any rate, it is merely noted that model selection for the model presented herein remains an open issue.

Finally, it is noted that using monthly and daily data might seem somewhat arbitrary and it could be argued that it would be better to use some aggregated data instead, e.g. monthly/daily maxima or mean. This could perhaps reduce the observed sensitivity of the results from changes in temporal resolution, but

the seasonal part might be less meaningful for e.g. monthly maxima. Notwithstanding, it is believed that the results are still valuable and provide useful insight in the long-term trends of significant wave height as well as on the performance of Bayesian hierarchical space-time models on data of varying temporal resolution.

7.1 Possible model extensions and future work

In order to provide long-term predictions related to climate change, evidence of which may yet not be present in the historical data, it may be necessary to include covariates in the model, where the covariates are chosen so that there exist reliable projections of the explanatory variables. Examples of such covariates could be fields of mean sea level pressure (as in [9]) or some measure of the level of greenhouse gases in the atmosphere, with projections based on various forcing scenarios [17].

Another alternative could be to include different temporal trends for different seasons. For example, four different temporal trends could be included to allow for different trends in spring, summer, autumn and winter seasons. It is believed that these trends could be significantly different, and that such a refinement could lead to better model performance. Furthermore, the model could incorporate a temporal trend in the variance (spread) of the data in order to account for heteroscedasticity beyond what was captured by the log-transform. It is acknowledged that changes in the extreme wave climate can result from a change in the variance even without a significant change in the mean. The combined effect of a change in the spread and the mean could be significant and an extended model incorporating a temporal long-term trend in the variance could yield interesting insight. Other possible extensions could be to allow the parameter b_0 to vary spatially or to try some other reasonable transformation of the data. Such, and other, model extensions have not been made to date and is left for future work. The model could also be fitted for data pertaining to different ocean areas to investigate whether it is able to capture different physical characteristics at different locations, but this is also left for future work.

8 Summary and conclusions

This paper has presented a Bayesian hierarchical space-time model for significant wave height data, with a log-transform, and applied it on a set of data extracted from ERA-40 for an area in the North Atlantic ocean, covering the period from 1958 to February 2002. Different temporal resolutions have been tried, illustrating the sensitivity of the model results to such changes. Five model alternatives have been considered, where the differences have been in how a long-term temporal trend is modelled and in the number of temporal noise terms (one or two). All model alternatives give similar results with respect to the spatial features of the model but the different models and different data resolutions yield slightly different estimates for the temporal features. The space-time dynamic term is seen to become increasingly important for increasing resolution, and different trend components obviously affects the estimated long-term trend. However, model selection remains inconclusive.

The trends estimated from the various simulations are fairly consistent, disregarding the simulations for six-hourly data, with estimated expected trends of 19 - 31 cm for moderate conditions and 63 - 100 cm for extreme conditions for the monthly data and 16 - 22 cm for moderate conditions and 55 - 73 cm for extreme conditions for the daily data over the period from 1958 - 2002. The linear trends were also extrapolated over 100 years, to yield expected increases within the range of 45 - 75 cm for moderate conditions and 1.5 - 2.5 m for extreme conditions. This is found to be in reasonable agreement with previous studies. It is also noted that the estimated trends for moderate sea states compare well with trends estimated without performing the logarithmic transformation of the data. However, whether the log-transform actually represents an improvement remains unclear.

Even though the model overall seems to perform quite well, it is noted that better insight and predictions may be obtained by extending the model. Possible model extensions could include covariates related to

meteorological data or emission scenarios or incorporate other features such as nonstationary noise terms. Such model extensions will be the focus of future research.

Acknowledgements

The authors want to express their thanks to Dr. Andreas Sterl at KNMI for kindly providing the data used in this analysis and for clarifying some issues discovered when investigating the data.

The simulations for the 6-hourly data, which were very computational intensive and time consuming, were performed on the Titan Cluster, owned by the University of Oslo and the Norwegian metacenter for High Performance Computing (NOTUR), and operated by the Research Computing Services group at USIT, the University of Oslo IT-department.

References

- [1] H. Akaike. A new look at the statistical model identification. *IEEE Transactions on Automatic Control*, 19:716–723, 1974.
- [2] A. V. Babanin, D. Chalikov, I. Young, and I. Savelyev. Numerical and laboratory investigation of breaking of steep two-dimensional waves in deep water. *Journal of Fluid Mechanics*, 644:433–463, 2010.
- [3] E. M. Bitner-Gregersen and C. de Valk. Quality control issues in estimating wave climate from hindcast and satellite data. In *Proc. 27th International Conference on Offshore Mechanics and Arctic Engineering (OMAE 2008)*. American Society of Mechanical Engineers (ASME), June 2008.
- [4] E. M. Bitner-Gregersen and Ø. Hagen. Uncertainties in data for the offshore environment. *Structural Safety*, 7:11–34, 1990.
- [5] G. J. Boer, G. Flato, M. C. Reader, and D. Ramsden. A transient climate change simulation with greenhouse gas and aerosol forcing: experimental design and comparison with the instrumental record for the twentieth century. *Climate Dynamics*, 16:405–425, 2000.
- [6] S. Caires and A. Sterl. 100-year return value estimates for ocean wind speed and significant wave height from the ERA-40 data. *Journal of Climate*, 18:1032–1048, 2005.
- [7] S. Caires and A. Sterl. A new nonparametric method to correct model data: Application to significant wave height from ERA-40 re-analysis. *Journal of Atmospheric and Oceanic Technology*, 22:443 – 459, 2005.
- [8] S. Caires and V. Swail. Global wave climate trend and variability analysis. In *Preprints of 8th International Workshop on Wave Hindcasting and Forecasting*, November 2004.
- [9] S. Caires, V. R. Swail, and X. L. Wang. Projection and analysis of extreme wave climate. *Journal of Climate*, 19:5581–5605, 2006.
- [10] N. Cressie and C. K. Wikle. *Statistics for Spatio-Temporal Data*. Wiley, 2011.
- [11] C. Cunha and C. Guedes Soares. On the choice of data transformation for modelling time series of significant wave height. *Ocean Engineering*, 26:489 – 506, 1999.
- [12] J. Debernard, Ø. Sætra, and L. P. Røed. Future wind, wave and storm surge climate in the northern North Atlantic. *Climate Research*, 23:39 – 49, 2002.
- [13] J. B. Debernard and L. P. Røed. Future wind, wave and storm surge climate in the Northern Seas: a revisit. *Tellus*, 60A:427–438, 2008.

- [14] I. Grabemann and R. Weisse. Climate change impact on extreme wave conditions in the North Sea: an ensemble study. *Ocean Dynamics*, 58:199 – 212, 2008.
- [15] IPCC. Climate change 2007: Synthesis report. Technical report, Intergovernmental Panel on Climate Change, 2007.
- [16] IPCC. *Climate Change 2007: The Physical Sciences Basis. Contribution of Working Group I to the Fourth Assessment Report of the Intergovernmental Panel on Climate Change*. Cambridge University Press, 2007.
- [17] N. Nakićenović, J. Alcamo, G. Davis, B. de Vries, J. Fenhann, S. Gaffin, K. Gregory, A. Grübler, T. Y. Jung, T. Kram, E. L. La Rovere, L. Michaelis, S. Mori, T. Morita, W. Pepper, H. Pitcher, L. Price, K. Riahi, A. Roehrl, H.-H. Rogner, A. Sankovski, M. Schlesinger, P. Shukla, S. Smith, R. Swart, S. van Rooijen, N. Victor, and Z. Dadi. *Emissions scenarios*. Cambridge University Press, 2000.
- [18] B. Natvig and I. F. Tvette. Bayesian hierarchical space-time modeling of earthquake data. *Methodology and Computing in Applied Probability*, 9:89–114, 2007.
- [19] K. Richardson, W. Steffen, H. J. Schellnhuber, J. Alcamo, T. Barker, D. M. Kammen, R. Leemans, D. Liverman, M. Munasinghe, B. Osman-Elasha, N. Stern, and O. Wæver. International scientific congress climate change: Global risks, challenges & decisions - synthesis report. Technical report, International Alliance of Research Universities, 2009.
- [20] C. P. Robert and G. Casella. *Monte Carlo Statistical Methods*. Springer, second edition, 2004.
- [21] G. Schwarz. Estimating the dimension of a model. *The Annals of Statistics*, 6:461–464, 1978.
- [22] D. J. Spiegelhalter, N. G. Best, B. P. Carlin, and A. van der Linde. Bayesian measures of model complexity and fit. *Journal of the Royal Statistical Society, Series B*, 64:583–639, 2002.
- [23] A. Sterl and S. Caires. Climatology, variability and extrema of ocean waves: The web-based KNMI/ERA-40 wave atlas. *International Journal of Climatology*, 25:963–977, 2005.
- [24] A. Toffoli, A. Babanin, M. Onorato, and T. Waseda. Maximum steepness of oceanic waves: Field and laboratory experiments. *Geophysical Research Letters*, 37:L05603, 2010.
- [25] S. M. Uppala, P. W. Kållberg, A. J. Simmons, U. Andrae, V. Da Costa Bechtold, M. Fiorino, J. K. Gibson, J. Haseler, A. Hernandez, G. A. Kelly, X. Li, K. Onogi, S. Saarinen, N. Sokka, R. P. Allan, E. Andersson, K. Arpe, M. A. Balmaseda, A. C. M. Beljaars, L. Van de Berg, J. Bidlot, N. Bormann, S. Caires, F. Chevallier, A. Dethof, M. Dragosavac, M. Fisher, M. Fuentes, S. Hagemann, B. J. Hólm, E. Hoskins, L. Isaksen, P. A. E. M. Janssen, R. Jenne, A. P. McNally, J.-F. Mahfouf, J.-J. Morcrette, N. A. Rayner, R. W. Saunders, P. Simon, A. Sterl, K. E. Trenberth, A. Untch, D. Vasiljevic, P. Vitebro, and J. Woolen. The ERA-40 re-analysis. *Quarterly Journal of the Royal Meteorological Society*, 131:2961–3012, 2005.
- [26] E. Vanem. Stochastic models for long-term prediction of extreme waves: a literature survey. In *Proc. 29th International Conference on Offshore Mechanics and Arctic Engineering (OMAE 2010)*. American Society of Mechanical Engineers (ASME), June 2010.
- [27] E. Vanem. Long-term time-dependent stochastic modelling of extreme waves. *Stochastic Environmental Research and Risk Assessment*, 25:185–209, 2011.
- [28] E. Vanem, A. B. Huseby, and B. Natvig. A Bayesian-hierarchical space-time model for significant wave height data. In *Proc. 30th International Conference on Offshore Mechanics and Arctic Engineering (OMAE 2011)*. American Society of Mechanical Engineers (ASME), June 2011.

- [29] E. Vanem, A. B. Huseby, and B. Natvig. A Bayesian hierarchical spatio-temporal model for significant wave height in the North Atlantic. *Stochastic Environmental Research and Risk Assessment*, in press, 2011.
- [30] X. J. Wang, F. W. Zwiens, and V. R. Swail. North Atlantic ocean wave climate change scenarios for the twenty-first century. *Journal of Climate*, 17:2368–2383, 2004.
- [31] X. L. Wang and V. R. Swail. Climate change signal and uncertainty in projections of ocean wave heights. *Climate Dynamics*, 26:109–126, 2006.
- [32] X. L. Wang and V. R. Swail. Historical and possible future changes of wave heights in northern hemisphere oceans. In W. Perrie, editor, *Atmosphere-Ocean Interactions*, volume 2 of *Advances in Fluid Mechanics*, Vol. 39, chapter 8, pages 185–218. WIT Press, 2006.
- [33] C. K. Wikle. Hierarchical models in environmental science. *International Statistical Review*, 71:181 – 199, 2003.
- [34] C. K. Wikle, L. M. Berliner, and N. Cressie. Hierarchical Bayesian space-time models. *Environmental and Ecological Statistics*, 5:117 – 154, 1998.
- [35] C. K. Wikle, R. F. Milliff, D. Nychka, and L. M. Berliner. Spatiotemporal hierarchical Bayesian modeling: Tropical ocean surface winds. *Journal of the American Statistical Association*, 96:382 – 397, 2001.
- [36] I. Young, S. Zieger, and A. Babanin. Global trends in wind speed and wave height. *Science*, 332:451–455, 2011.